Neurochem Res (2016) 41:2367–2379
DOI 10.1007/s11064-016-1950-9

ORIGINAL PAPER

Resveratrol Attenuates $A\beta_{25–35}$ Caused Neurotoxicity by Inducing Autophagy Through the TyrRS-PARP1-SIRT1 Signaling Pathway

Haoyue Deng[1] · **Man-tian Mi**[1]

Received: 28 March 2016 / Revised: 3 May 2016 / Accepted: 6 May 2016 / Published online: 14 May 2016

Abstract Alzheimer's disease (AD) is a neurodegenerative disorder characterized by the accumulation of β-amyloid peptide (Aβ) and loss of neurons. Resveratrol (RSV) is a natural polyphenol that has been found to be beneficial for AD through attenuation of Aβ-induced toxicity in neurons both in vivo and in vitro. However, the specific underlying mechanisms remain unknown. Recently, autophagy was found to protect neurons from toxicity injuries via degradation of impaired proteins and organelles. Therefore, the aim of this study was to determine the role of autophagy in the anti-neurotoxicity effect of RSV in PC12 cells. We found that RSV pretreatment suppressed β-amyloid protein fragment 25–35 ($A\beta_{25–35}$)-induced decrease in cell viability. Expression of light chain 3-II, degradation of sequestosome 1, and formation of autophagosomes were also upregulated by RSV. Suppression of autophagy by 3-methyladenine abolished the favorable effects of RSV on $A\beta_{25–35}$-induced neurotoxicity. Furthermore, RSV promoted the expression of sirtuin 1 (SIRT1), auto-poly-ADP-ribosylation of poly (ADP-ribose) polymerase 1 (PARP1), as well as tyrosyl transfer-RNA (tRNA) synthetase (TyrRS). Nevertheless, RSV-mediated autophagy was markedly abolished with the addition of inhibitors of SIRT1 (EX527), nicotinamide phosphoribosyltransferase (STF-118804), PARP1 (AG-14361), as well as *SIRT1* and *TyrRS* small interfering RNA transfection, indicating that the action of RSV on autophagy induction was dependent on TyrRS, PARP1 and SIRT1. In conclusion, RSV attenuated neurotoxicity caused by $A\beta_{25–35}$ through inducing autophagy in PC12 cells, and the autophagy was partially mediated via activation of the TyrRS-PARP1-SIRT1 signaling pathway.

Keywords $A\beta_{25–35}$ · Autophagy · Neurotoxicity · Resveratrol · TyrRS

Abbreviations

3-MA	3-methyladenine
AD	Alzheimer's disease
Aβ	β-amyloid peptide
$A\beta_{25–35}$	β-amyloid protein fragment 25–35
CCK-8	Cell counting kit-8
LC3	Light chain 3
NAD^+	Nicotinamide adenine dinucleotide
NAMPT	Nicotinamide phosphoribosyltransferase
PARP1	Auto-poly-ADP-ribosylation of poly (ADP-ribose) polymerase 1
p62	Sequestosome 1
RSV	Resveratrol
siRNA	Small interfering RNA
SIRT1	Sirtuin 1
TyrRS	Tyrosyl transfer-RNA (tRNA) synthetase

Introduction

Alzheimer's disease (AD) is an aged-related neurodegenerative disease characterized by the accumulation of β-amyloid peptide (Aβ) and loss of neurons [1, 2]. As a virulence factor, abnormal Aβ aggregation plays a vital role in the initiation phase of AD pathogenesis [3]. Therefore, reducing Aβ protein toxicity and inhibiting Aβ

✉ Man-tian Mi
mantianmi2012@163.com

[1] Research Center for Nutrition and Food Safety, Institute of Military Preventive Medicine, Third Military Medical University, 30th Gaotanyan Main Street, Shapingba District, Chongqing 400038, People's Republic of China

oligomer formation have been considered as potential therapeutic targets for AD prevention and treatment [4]. Epidemiological studies have suggested that many polyphenols naturally present in fruits and vegetables exert excellent health protective effects, which may be potential candidates for the prevention and treatment of AD [5]. Resveratrol (3, 4′, 5-trihydroxystilbene, RSV) is a natural polyphenol that has been found to be beneficial for AD through attenuation of Aβ-induced toxicity in neurons both in vivo and in vitro [6–9]. However, the underlying mechanism remains to be elucidated.

Autophagy is a catabolic process for the degradation and recycling of macromolecules and organelles [10]. Recently, autophagy has been found to be beneficial in the context of aging and various models of neurodegenerative diseases, including AD [11, 12]. Genetic analysis of samples from AD patients has shown that Beclin 1, a key protein in autophagy induction, is reduced in AD patients, which could be one of the earliest causes of autophagy dysregulation in AD [13]. Meanwhile, genome-wide screening analysis showed upregulation of the transcriptional levels of many other genes related to autophagy induction, probably as a compensatory mechanism in response to autophagy impairment [14]. Given these observations, autophagy as a potential therapeutic target in AD is receiving more and more attention. Furthermore, RSV was found to attenuate the fitness of various cells under conditions of metabolic stress and promote longevity via triggering autophagy [15–17]. In the presence of autophagy inhibitors or small interfering RNAs (siRNAs), the protective effects of RSV are lost, indicating that autophagy is required for the cytoprotective effects of RSV [15–17]. Thus, the aim of this study was to explore whether autophagy was essential in the beneficial effect of RSV on Aβ-induced neurotoxicity.

Sirtuin 1 (SIRT1), an important member of the silent information regulator 2 family, has an essential role in protecting against AD [18–20]. Recently, SIRT1 was shown to act as a positive regulator of basal autophagy through modulating the expression of several autophagy-related proteins [21]. Meanwhile, SIRT1-dependent autophagy activation has been found to be necessary for the benefits of RSV on aging-related diseases [22]. Our previous studies have found that RSV attenuated endothelial inflammation and hepatic steatosis through the SIRT1/autophagy signaling pathway [23, 24]. However, it was recently demonstrated that RSV did not activate SIRT1 directly. In 2014, Sajish and Schimmel [25] found that tyrosyl transfer-RNA (tRNA) synthetase (TyrRS) is the direct biological target of RSV. RSV can directly bind to the active site of TyrRS, thereafter nullifying the catalytic activity of TyrRS and redirecting it to a nuclear function, thereby stimulating nicotinamide adenine dinucleotide (NAD^+)-dependent auto-poly-ADP-ribosylation of poly(-ADP-ribose) polymerase 1 (PARP1), ultimately resulting in SIRT1 activation. Thus, we hypothesized that RSV may induce autophagy in response to neurotoxicity induced by β-amyloid protein fragment 25–35 ($A\beta_{25–35}$) via the TyrRS-PARP1-SIRT1 signaling pathway. To confirm this hypothesis, we investigated the effects of RSV on autophagy induction at different doses following $A\beta_{25–35}$-stimulation and the potential role of autophagy in preventing $A\beta_{25–35}$-induced neurotoxicity after RSV pretreatment in PC12 cells. Furthermore, the potential involvement of the TyrRS-PARP1-SIRT1 signaling pathway was also investigated.

Our results demonstrated, for the first time, that RSV ameliorated $A\beta_{25–35}$-induced neurotoxicity by activating autophagy via the TyrRS-PARP1-SIRT1 signaling pathway, which may open new avenues to develop novel drugs for the prevention of AD.

Materials and Methods

Antibodies and Reagents

Cell culture media high-glucose Dulbecco's modified Eagle's medium (DMEM, JP01117785) and fetal bovine serum (SH30370.03) were purchased from HyClone Laboratories, Inc. (Logan, UT, USA). Cell Counting kit-8 (CCK-8, CK04) was purchased from Dojindo Molecular Technologies, Inc. (Kumamoto, Japan). $A\beta_{25–35}$ (A4559), 3-methyladenine (3-MA, M9281), dimethyl sulfoxide (D2650), EX527 (E7034), light chain 3 (LC3, L7543), and RSV (R5010) were purchased from Sigma–Aldrich Corporation (St. Louis, MO, USA). Antibodies for TyrRS (ab50961) and sequestosome 1 (p62, ab56416) were purchased from Abcam Plc (Cambridge, MA, USA). PARP1 (9532S) and SIRT1 (8469S) antibodies were purchased from Cell Signaling Technology, Inc. (Beverly, MA, USA). STF-118804 (S7316) and AG-14361 (S2178) were purchased from Selleck Chemicals (Houston, TX, USA). *TyrRS* siRNA (sc-37672) and *SIRT1* siRNA (sc-40987) were purchased from Santa Cruz Biotechnology, Inc. (Santa Cruz, CA, USA). Antibody against β-actin (wbb-2101) was purchased from BestBio Biotechnology Co., Ltd. (Shanghai, China). Lipofectamine™ 2000 transfection reagent (11668-019) was purchased from Invitrogen Corporation (Carlsbad, CA, USA).

Pretreatment of $A\beta_{25–35}$

$A\beta_{25–35}$ was prepared as previously described [26]. Briefly, 1 mg $A\beta_{25–35}$ was dissolved in 188.6 μL of high-temperature sterilized distilled water (2.5 mM) and then stored at

−20 °C. The working solution was prepared with serum-free DMEM to the desired concentration and subsequently aged by incubation at 37 °C for 7 days before use.

Cell Culture and Treatment

Differentiated PC12 cells (differentiated with 50 ng/mL nerve growth factor in serum-free DMEM for 3 days), purchased from the Cell Resource Center of Shanghai Institutes for Biological Sciences, Chinese Academy of Sciences (Shanghai, China), were cultured in high-glucose DMEM supplemented with 10 % fetal bovine serum and penicillin (100 U/mL)/streptomycin sulfate (100 μg/mL) (Invitrogen Corporation) at 37 °C in a humidified atmosphere of 5 % CO_2. All experiments were performed once the cells reached 80–90 % confluence.

During the logarithmic growth phase, cells were treated in the presence or absence of 5 mM 3-MA (a specific inhibitor of autophagy), 2 μM EX527 (a selective inhibitor of SIRT1), 100 nM STF-118804 (a highly specific nicotinamide phosphoribosyltransferase (NAMPT) inhibitor), or 10 μM AG-14361 (an effective inhibitor of PARP1) for 1 h, before the addition of RSV (20 μM) for 2 h. Thereafter, the cells were treated with 30 μM $A\beta_{25–35}$ for another 24 h. To avoid starvation-induced autophagy, all treatments were performed in complete culture medium.

Cell Viability Measurement

The CCK-8 detection kit was used to measure cell viability as previously described [27]. Briefly, PC12 cells were seeded in a 96-well microplate (catalog no. 3650; Corning Life Sciences, Corning, NY, USA) at a density of 15,000 cells/well. Subsequently, 10 μL of CCK-8 solution was added to each well, then the plate was incubated at 37 °C for 2 h. Viable cells were counted by absorbance measurements with a multifunctional microplate reader (Spectra Max M2; Molecular Devices, LLC, Sunnyvale, CA, USA) at a wavelength of 450 nm. The optical density value at 450 nm was reported as the percentage of cell viability in relation to the control group (set as 100 %).

Western Blot Analysis

Total cell lysate was analyzed by western blot analysis as previously described [28]. Briefly, total protein content was extracted and protein concentration was determined using a BCA kit (Beyotime Institute of Biotechnology, Shanghai, China). The proteins (30–50 μg) were resolved by 10 % or 15 % SDS-PAGE, and then electro-blotted onto polyvinylidene difluoride membranes in an ice-water environment. Blots were blocked with 5 % defatted milk (Boster Biological Technology, Wuhan, China) in Tris-buffer and then probed with 1:1000-diluted primary antibodies overnight at 4 °C, followed by horseradish peroxidase-conjugated secondary antibodies (catalog nos. 31340 and 31455; Thermo Scientific Lab Vision, Fremont CA, USA). Then, the proteins were visualized by addition of ECL reagent (Millipore Corporation, Billerica, MA, USA) and exposure using a multifunction imager (Fusion FX, Vilber Lourmat Deutschland GmbH, Eberhardzell, Germany). Finally, the blots were scanned and densitometric analysis of the scanned images was performed using Scion Image-Release Beta 4.02 software (http://scion-corporation.software.informer.com/).

siRNA Assay

TyrRS siRNA (sc-37672), *SIRT1* siRNA (sc-40987) and control siRNA (sc-44230) were purchased from Santa Cruz Biotechnology. Lipofectamine™ 2000 was diluted in reduced serum DMEM according to the manufacturer's protocol. The final siRNA concentration was 60 nM. PC12 cells were transfected for 5–7 h, then the cells were incubated in DMEM medium for an additional 24 h. Where indicated, cells were treated with RSV (20 μM) for 2 h and then exposed to 30 μM of $A\beta_{25–35}$ for another 24 h. Thereafter, cells were harvested and western blot analysis was performed.

Transmission Electron Microscopy

PC12 cells were collected and fixed in 2 % paraformaldehyde and 0.1 % glutaraldehyde in 0.1 M sodium cacodylate for 2 h, post-fixed with 1 % OsO_4 for 1.5 h, washed, and stained for 1 h in 3 % aqueous uranyl acetate. The samples were then washed again, dehydrated with graded alcohol, and embedded in Epon-Araldite resin (catalog no. 034; Canemco & Marivac, Gore, QC, Canada). Ultrathin sections were cut on a ultramicrotome (Reichert-Jung MicroStar Series; Ametek Reichert Technologies, Depew, NY, USA), counterstained with 0.3 % lead citrate, and examined using a transmission electron microscope (model: JEM-1400Plus; JEOL, Tokyo, Japan).

Statistical Analyses

SPSS 13.0 software (SPSS Inc., Chicago, IL, USA) was used for statistical analysis. CCK-8 and densitometric data were processed by analysis of variance. Quantitative data are presented as means ± standard deviations (SD) of the experiments. A probability (p) value <0.05 was considered statistically significant.

Results

RSV Attenuated $A\beta_{25–35}$-Induced Neurotoxicity in PC12 Cells

According to previous observations, cells were treated with different concentrations of $A\beta_{25–35}$ (10, 20, 30, 40, and 80 μM) for 24 h. As indicated in Fig. 1a, $A\beta_{25–35}$ decreased cell viability in a dose-dependent manner. Cell viability was reduced to 53.45 ± 0.60 % when treated with 30 μM $A\beta_{25–35}$ for 24 h compared to the control group. Meanwhile, PC12 cells were incubated with various concentrations of RSV (0.1, 1, 2.5, 5, 10, 20, 50, 100, and 200 μM) to investigate cytotoxicity. RSV at concentrations of up to 50 μM was tolerated by PC12 cells without a significant effect on cell viability (Fig. 1b). Thus, cells were pre-incubated with RSV (1, 5, 10, and 20 μM) for 2 h, and then exposed to 30 μM $A\beta_{25–35}$ for an additional 24 h in our subsequent experiments. $A\beta_{25–35}$-treated cells swelled and assumed round shapes along with cell debris, which was reversed by the addition of RSV (Fig. 1c). Moreover, RSV pretreatment significantly attenuated the detrimental effect of $A\beta_{25–35}$ on viability of PC12 cells (Fig. 1d). These results indicated that RSV pretreatment remarkably attenuated $A\beta_{25–35}$-induced injury in PC12 cells.

RSV Attenuated $A\beta_{25–35}$-Caused Neurotoxicity by Inducing Autophagy in PC12 Cells

Expression of protein LC3-II and p62, indicators of autophagy, was detected by western blotting. RSV-single treatment notably up-regulated LC3-II expression and p62 degradation in a dose-dependent manner (Fig. 2a–c). Furthermore, similar results were found in the RSV and $A\beta_{25–35}$ co-treated group (Fig. 2d–f). To further demonstrate RSV-induced autophagy in $A\beta_{25–35}$-stimulated PC12 cells, the role of RSV in autophagosome formation was investigated. As confirmed by transmission electron microscopy, RSV promoted autophagosome formation in $A\beta_{25–35}$-treated PC12 cells. Nevertheless, pretreatment with 5 mM 3-MA (an inhibitor of the early autophagy stage) remarkably decreased RSV-mediated autophagosome formation (Fig. 2g). Meanwhile, RSV-induced expression of LC3-II and degradation of p62 was markedly inhibited in the presence of 3-MA in $A\beta_{25-35}$-stimulated

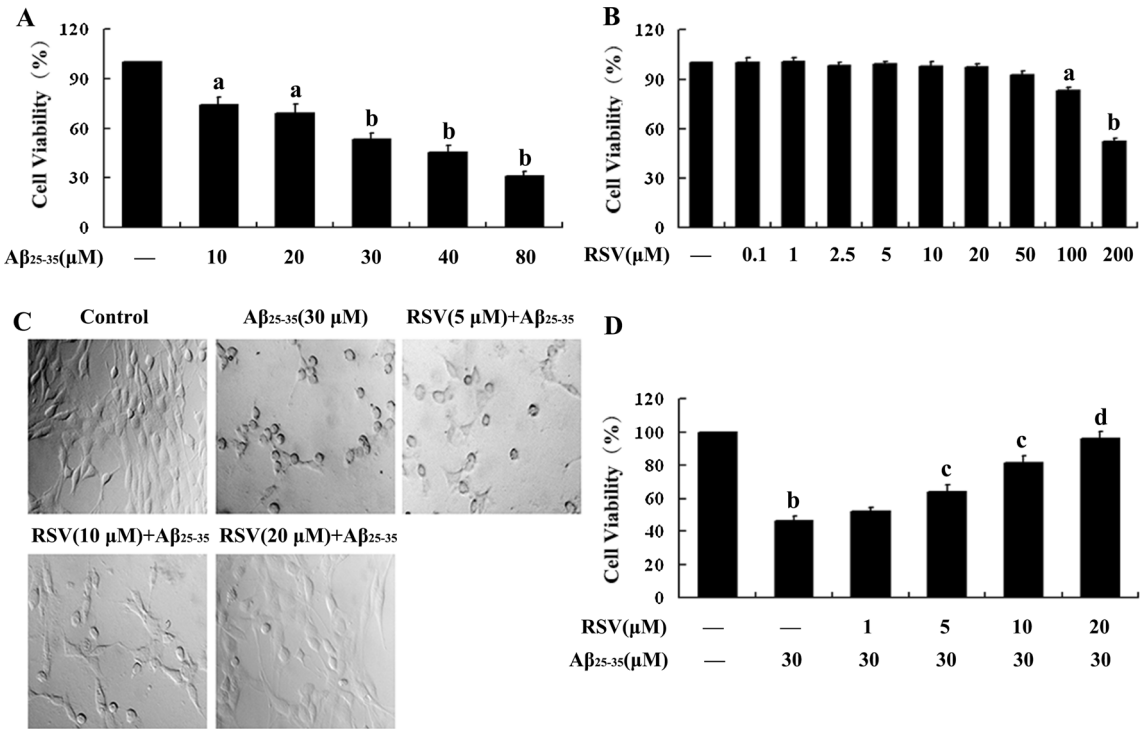

Fig. 1 RSV attenuated $A\beta_{25–35}$-induced cytotoxicity in PC12 cells. **a** Cells were incubated with different concentrations of $A\beta_{25–35}$ (10, 20, 30, 40, and 80 μM) for 24 h. Subsequently, cell viability was measured using a CCK-8 detection kit, as described in the "Materials and Methods" section. **b** Cells were treated with different concentrations (0.1, 1, 2.5, 5, 10, 20, 50, 100, and 200 μM) of RSV for 24 h and cell viability was measured using the CCK-8 detection kit. PC12 cells were pretreated with different concentrations (1, 5, 10, and 20 μM) of RSV followed by treatment with or without $A\beta_{25–35}$ (30 μM) for an additional 24 h. **c** Cells were visualized under a microscope at ×400 magnification. **d** Cell viability was detected using the CCK-8 detection kit. Values are presented as mean ± SD (n = 3); $^{a}p < 0.05$; $^{b}p < 0.01$ versus the vehicle-treated control group; $^{c}p < 0.05$; $^{d}p < 0.01$ versus $A\beta_{25–35}$-treated group

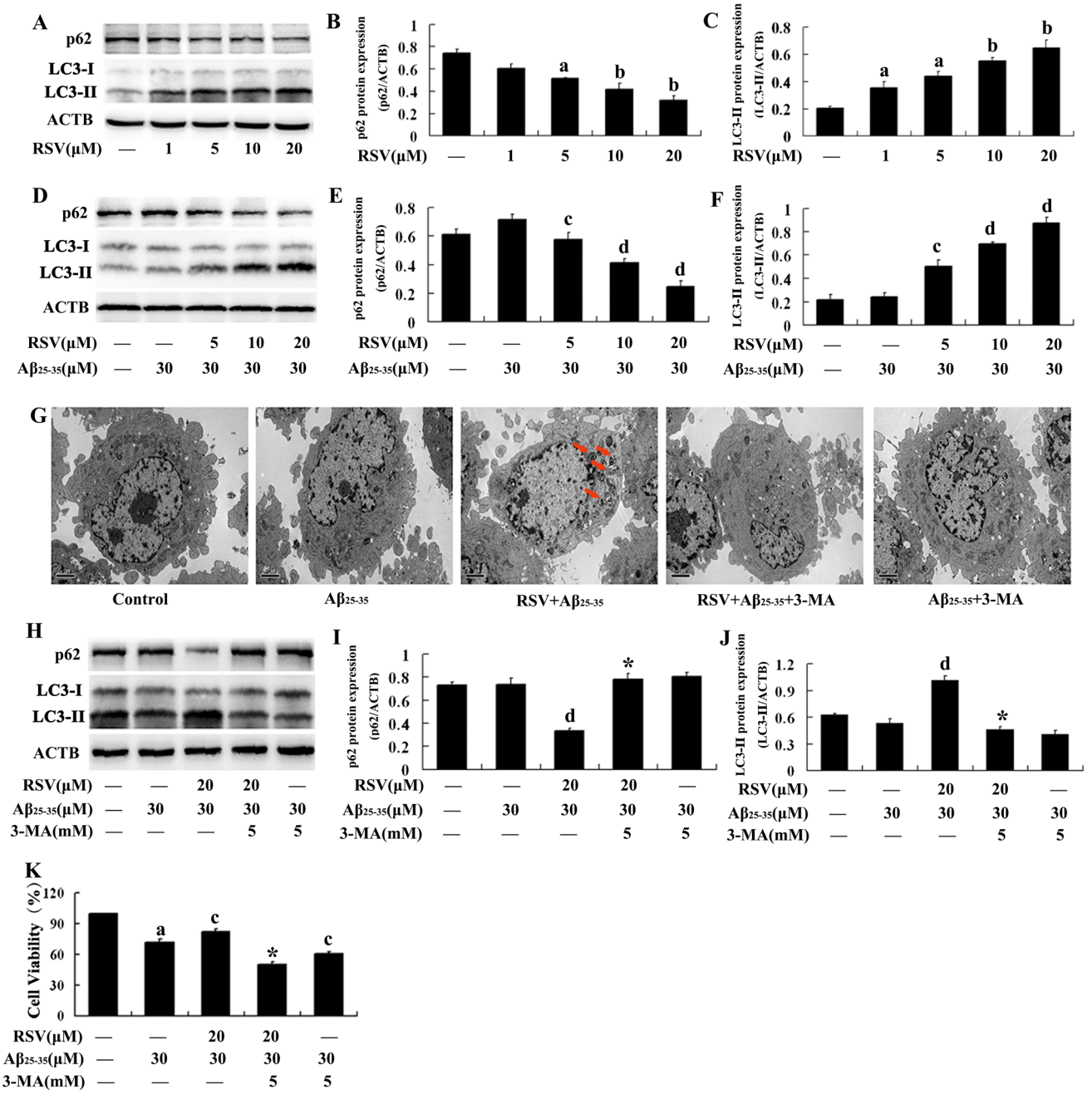

Fig. 2 RSV attenuated $A\beta_{25–35}$-induced neurotoxicity by promoting autophagy in PC12 cells. **a** RSV increased LC3-II formation and p62 degradation in PC12 cells. Cells were treated with RSV at a series of concentrations (1, 5, 10, and 20 μM) and the expression levels of p62 and LC3-II were detected by western blot analysis. **b**, **c** *Bar charts* show the quantification of endogenous p62 and LC3-II. PC12 cells were pretreated with different concentrations (1, 5, 10, and 20 μM) of RSV followed by treatment with or without $A\beta_{25–35}$ (30 μM) for an additional 24 h. **d** p62 and LC3-II expression was detected by western blot analysis. **e**, **f** *Bar charts* show the quantification of endogenous p62 and LC3-II. Cells were pretreated with 3-MA (5 mM) for 1 h prior to treatment with RSV (20 μM) for another 2 h, followed by treatment with or without $A\beta_{25–35}$ (30 μM) for an additional 24 h. **g** Representative transmission electron microscopic images of cells with *arrows* indicating autophagosomes. **h** Expression of p62 and LC3-II was analyzed by western blot analysis. **i**, **j** *Bar charts* show the quantification of the indicated proteins. **k** Cell viability was measured using the CCK-8 detection kit. Values are presented as mean ± SD (n = 3); $^{a}p < 0.05$; $^{b}p < 0.01$ versus the vehicle-treated control group; $^{c}p < 0.05$; $^{d}p < 0.01$ versus $A\beta_{25–35}$-treated group; $^{*}p < 0.01$ versus RSV and $A\beta_{25–35}$ co-treated group

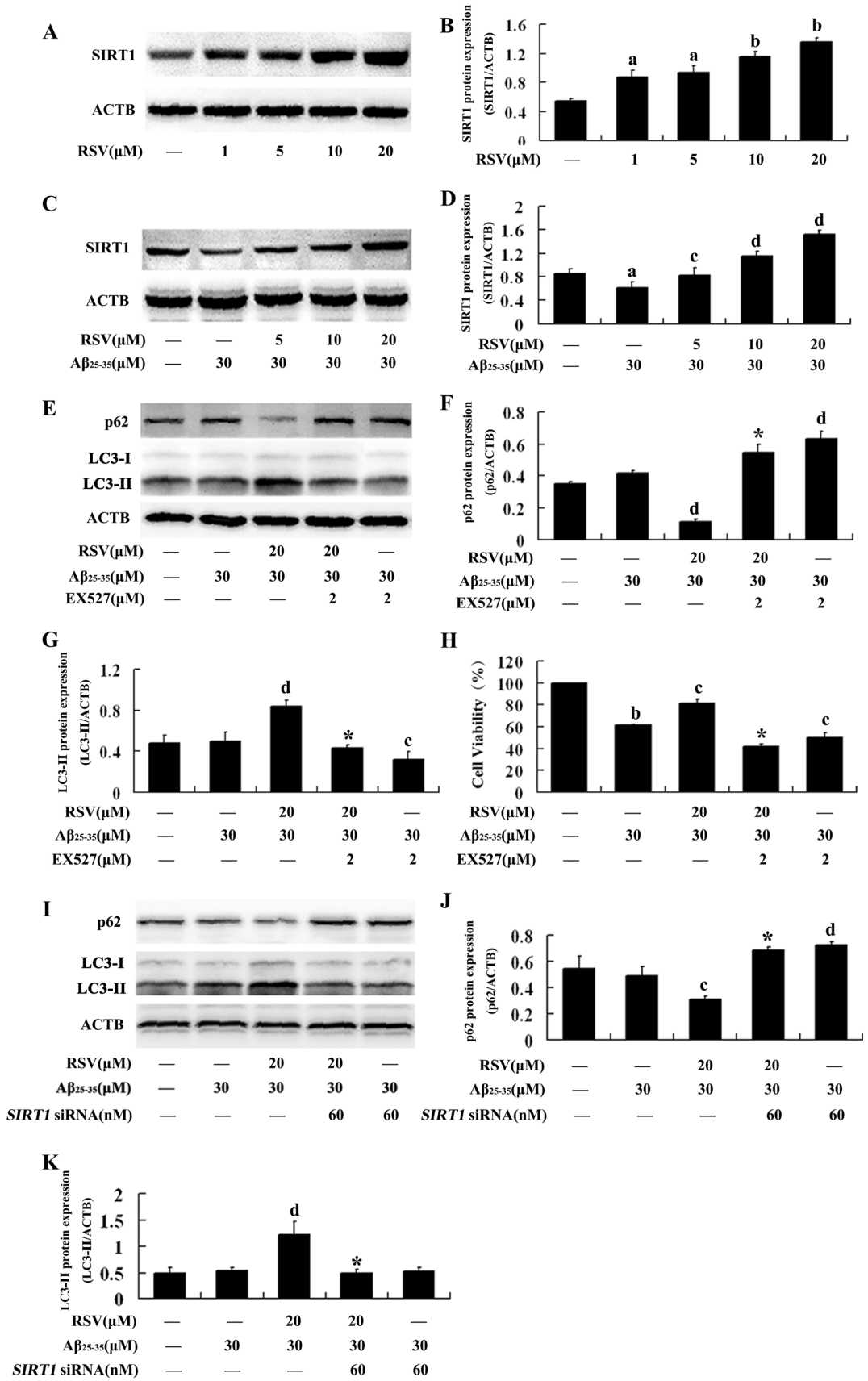
A
SIRT1
ACTB
RSV(μM) — 1 5 10 20
B
SIRT1 protein expression (SIRT1/ACTB)
1.6
1.2
0.8
0.4
0
a a b b
RSV(μM) — 1 5 10 20
C
SIRT1
ACTB
RSV(μM) — — 5 10 20
Aβ25-35(μM) — 30 30 30 30
D
SIRT1 protein expression (SIRT1/ACTB)
2
1.6
1.2
0.8
0.4
0
a c d d
RSV(μM) — — 5 10 20
Aβ25-35(μM) — 30 30 30 30
E
p62
LC3-I
LC3-II
ACTB
RSV(μM) — — 20 20 —
Aβ25-35(μM) — 30 30 30 30
EX527(μM) — — — 2 2
F
p62 protein expression (p62/ACTB)
0.8
0.6
0.4
0.2
0
d * d
RSV(μM) — — 20 20 —
Aβ25-35(μM) — 30 30 30 30
EX527(μM) — — — 2 2
G
LC3-II protein expression (LC3-II/ACTB)
1.2
0.8
0.4
0
d * c
RSV(μM) — — 20 20 —
Aβ25-35(μM) — 30 30 30 30
EX527(μM) — — — 2 2
H
Cell Viability (%)
120
100
80
60
40
20
0
b c * c
RSV(μM) — — 20 20 —
Aβ25-35(μM) — 30 30 30 30
EX527(μM) — — — 2 2
I
p62
LC3-I
LC3-II
ACTB
RSV(μM) — — 20 20 —
Aβ25-35(μM) — 30 30 30 30
SIRT1 siRNA(nM) — — — 60 60
J
p62 protein expression (p62/ACTB)
0.8
0.6
0.4
0.2
0
c * d
RSV(μM) — — 20 20 —
Aβ25-35(μM) — 30 30 30 30
SIRT1 siRNA(nM) — — — 60 60
K
LC3-II protein expression (LC3-II/ACTB)
2
1.5
1
0.5
0
d *
RSV(μM) — — 20 20 —
Aβ25-35(μM) — 30 30 30 30
SIRT1 siRNA(nM) — — — 60 60

◀**Fig. 3** RSV-induced autophagy in a SIRT1-dependent manner in PC12 cells. **a** Cells were treated with various concentrations (1, 5, 10, and 20 μM) of RSV for 24 h. SIRT1 expression was detected by western blot analysis. **b** The *bar graph* shows the quantification of endogenous SIRT1. **c** Cells were pretreated with RSV at different concentrations (5, 10, and 20 μM) and then exposed to $A\beta_{25-35}$ (30 μM) for an additional 24 h. SIRT1 expression was detected by western blot analysis. **d** The *bar graph* shows the quantification of endogenous SIRT1. Cells were pretreated with EX527 (2 μM) for 1 h prior to treatment with RSV (20 μM) for another 2 h. Thereafter, cells were incubated in the presence or absence of $A\beta_{25-35}$ (30 μM) for an additional 24 h. **e** Expression of p62 and LC3-II was determined by western blot analysis. **f**, **g** The bar graphs show the quantification of endogenous p62 and LC3-II. **h** Cell viability was measured using the CCK-8 assay. **i** Cells were transfected with *SIRT1* siRNA (60 nM) for 5–7 h as described in the "Materials and Methods" section. At 24 h post-transfection, the cells were pretreated with RSV (20 μM) for 2 h and then incubated in the presence or absence of $A\beta_{25-35}$ (30 μM) for an additional 24 h. Expression of p62 and LC3-II was detected by western blot analysis. **j**, **k** The *bar graphs* show the quantification of endogenous p62 and LC3-II. Values are presented as mean ± SD (n = 3); $^{a}p < 0.05$; $^{b}p < 0.01$ versus the vehicle-treated control group; $^{c}p < 0.05$; $^{d}p < 0.01$ versus $A\beta_{25-35}$-treated group;$^{*}p < 0.01$ versus RSV and $A\beta_{25-35}$ co-treated group

PC12 cells (Fig. 2h–j). These results suggest that autophagy was evidently induced by RSV in $A\beta_{25-35}$-treated PC12 cells.

Additionally, when autophagy was inhibited by 3-MA, the RSV-induced increase in viability of PC12 cells was significantly inhibited by $A\beta_{25-35}$ treatment (Fig. 2k). These results indicated that RSV attenuated $A\beta_{25-35}$-induced neurotoxicity by activating autophagy.

RSV-Induced Autophagy was SIRT1-Dependent in PC12 Cells

We further investigated the mechanism of RSV-induced autophagy in PC12 cells. As known, SIRT1 is a molecular target of RSV [29]; therefore, correlations of autophagy induction and RSV-mediated SIRT1 activation in PC12 cells were explored. Our results revealed that single treatment of RSV increased SIRT1 expression dose-dependently in PC12 cells (Fig. 3a, b). Similar results were observed in RSV and $A\beta_{25-35}$ co-treated cells (Fig. 3c, d). Moreover, the SIRT1 inhibitor EX527 and *SIRT1* siRNA were used to determine the role of the SIRT1 signaling pathway. As indicated in Fig. 3e–g, EX527 (2 μM) pretreatment inhibited RSV-induced autophagy, as evidenced by the increase in p62 level and decrease in LC3-II expression in $A\beta_{25-35}$-treated PC12 cells. In addition, RSV remarkably alleviated the decrease in cell viability induced by $A\beta_{25-35}$, which was also inhibited by EX527 (Fig. 3h). Similar results were observed when the *SIRT1* gene was suppressed by *SIRT1* siRNA transfection (Fig. 3i–k).These results indicated that RSV-induced autophagy was SIRT1-dependent in PC12 cells.

RSV Activated SIRT1 Expression via the TyrRS-PARP1 Pathway in PC12 Cells

Intracellular NAD^+ levels control the activity of the type III deacetylase SIRT1 [30]. Therefore, we further explored the role of NAD^+ in RSV-induced SIRT1 expression. As shown in Fig. 4a and b, RSV notably promoted the expression of SIRT1; however, this effect was significantly abolished by STF-118804 (100 nM), a unique inhibitor of NAMPT, which is the rate-limiting enzyme converting nicotinamide to NAD^+ [31]. These outcomes reflected the importance of NAD^+ in RSV-mediated SIRT1 expression. Since PARP1 is the major regulator of NAD^+ metabolism and its related signaling pathway [32], thereafter we investigated the role of PARP1 in RSV-induced SIRT1 expression. As expected, RSV markedly up-regulated PARP1 expression in a dose-dependent manner in PC12 cells treated with or without $A\beta_{25-35}$ (Fig. 4c–f). Subsequently, we added a potent PARP1 inhibitor (AG14361, 10 μM) to further confirm the involvement of PARP1 in $A\beta_{25-35}$-treated PC12 cells. As shown in Fig. 4g–i, RSV-induced expression of SIRT1 was down-regulated by AG14361, suggesting that PARP1 was required for RSV activation of SIRT1.

Recent report demonstrates that RSV could directly bind to the active site of TyrRS, resulting in stimulating PARP1 and ultimately activating NAD^+-dependent SIRT1 [25]. Herein, we also examined the possible role of TyrRS in RSV-induced PARP1 expression. Single-RSV treatment increased TyrRS in a dose-dependent manner as monitored by western blotting (Fig. 5a, b). Similar results were found with RSV and $A\beta_{25-35}$ co-treatment (Fig. 5c, d). However, when *TyrRS* gene was suppressed by *TyrRS* siRNA (60 nM) transfection, the effect of RSV on TyrRS expression was markedly diminished, leading to the down-regulation of PARP1 in PC12 cells (Fig. 5e–g). Together, we concluded that the TyrRS-PARP1 pathway was crucial for SIRT1 activation and subsequent RSV-mediated autophagy in $A\beta_{25-35}$-stimulated PC12 cells.

Discussion

AD is hidden onset and possesses a long incubation period. It is a devastating disorder presenting a huge life-style and economic burden to both the patients and their families [1, 2]. Currently, the prevalence of AD doubles every 5 years after the age of 65, affecting nearly one-eighth of people older than 65 years [1, 2]. The number of patients with AD is expected to reach 30 million worldwide by 2050 [33]. Deposits of hyperphosphorylated tau and Aβ are primary pathologic hallmarks of AD, which lead, respectively, to the formation of neurofibrillary tangles and neuronal

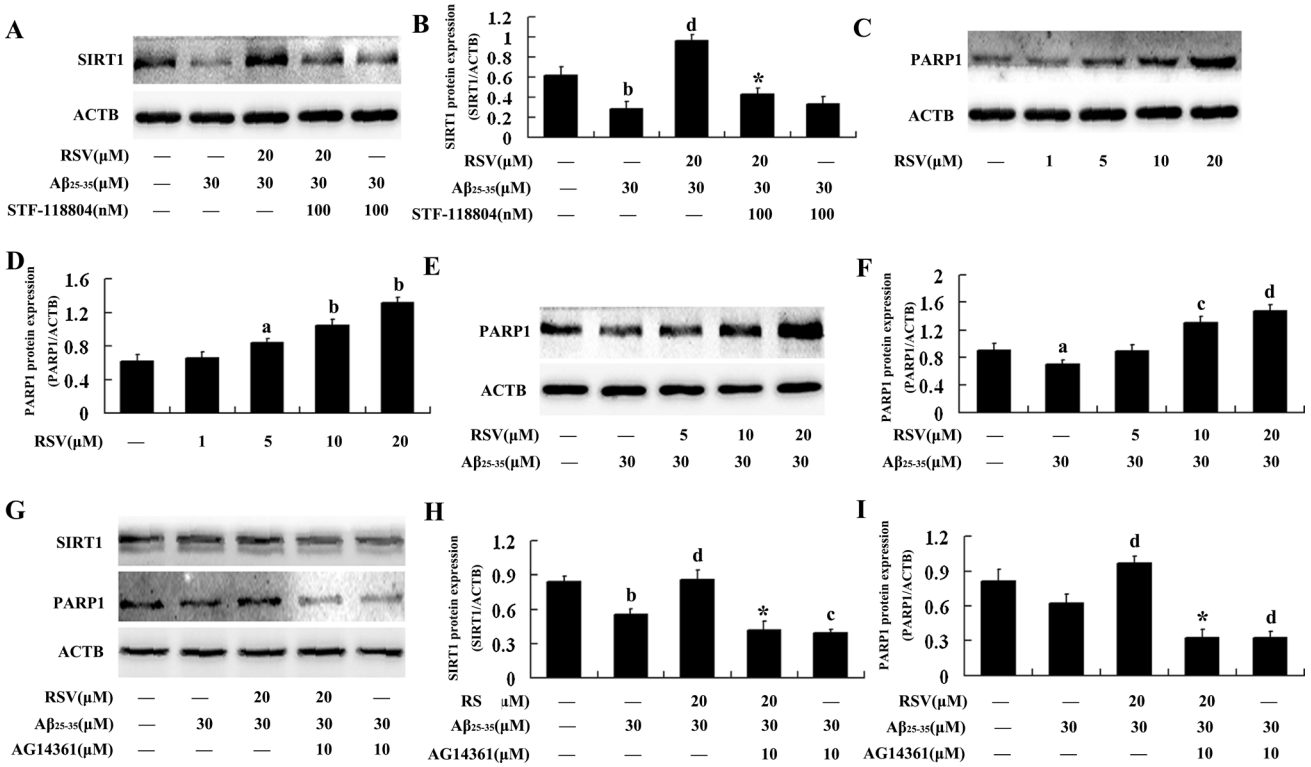

Fig. 4 RSV-induced SIRT1 expression is PARP1-dependent in PC12 cells. **a** PC12 cells were pretreated with STF-118804 (100 nM) for 1 h prior to treatment with RSV (20 μM) for another 2 h, followed by treatment with or without of $A\beta_{25–35}$ (30 μM) for an additional 24 h. SIRT1 expression was determined by western blot analysis. **b** The *bar graph* shows the quantification of endogenous SIRT1. **c** Cells were treated with various concentrations (1, 5, 10, and 20 μM) of RSV for 24 h. PARP1 expression was detected by western blot analysis. **d** The *bar graph* shows the quantification of endogenous PARP1. **e** Cells were pretreated with RSV at different concentrations (5, 10 and 20 μM), then, cells were exposed to $A\beta_{25–35}$ (30 μM) for an additional 24 h. PARP1 expression was detected by western blot analysis. **f** The *bar graph* shows the quantification of endogenous PARP1. **g** Cells were pretreated with AG14361 (10 μM) for 1 h prior to treatment with RSV (20 μM) for another 2 h, followed by treatment with or without of $A\beta_{25–35}$ (30 μM) for an additional 24 h. Expression of SIRT1 and PARP1 was determined by western blot analysis. **h**, **i** *Bar graphs* show the quantification of endogenous SIRT1 and PARP1. Values are presented as mean ± SD (n = 3); $^{a}p < 0.05$; $^{b}p < 0.01$ versus the vehicle-treated control group; $^{c}p < 0.05$; $^{d}p < 0.01$ versus $A\beta_{25–35}$-treated group; $^{*}p < 0.01$ versus RSV and $A\beta_{25-35}$ co-treated group

plaques [34]. Pharmaceutical and dietary strategies have targeted these disorders to control AD, and many natural products with excellent pharmacological properties are good candidates for the control or prevention of AD [5]. RSV is a polyphenolic compound with obvious antioxidant, anti-aging, and anti-inflammatory properties [35, 36]. Recently, intense efforts have focused on the use of RSV to promote longevity and neuronal protection [34]. On account of the property to readily pass through the blood brain barrier, after entering the blood stream and conjugating with glucuronide, RSV plays a prominent role in the prevention of neurodegenerative disorders such as Parkinson's disease, Huntington's disease, as well as AD [8, 9]. Bastianetto et al. [37] suggested that RSV could inhibit the aggregation of protein Aβ and adjust survival and apoptosis of nerve cells. Simultaneously, Pasinetti et al. [5] indicated that polyphenols selected from red wines, including RSV, may alleviate AD by modulating Aβ through inhibition of both generation and oligomerization of Aβ, as well as promoting Aβ clearance. Recently, it has been found that RSV attenuated Aβ-induced toxicity in neurons both in vivo and in vitro [6–9]. However, the specific underlying mechanism remains unknown.

In the current study, we, for the first time, demonstrated that RSV could attenuate $A\beta_{25-35}$-caused neurotoxicity by autophagy induction. Autophagy, widely exists in eukaryotic cells, is a cellular degradation pathway of proteins and organelles [38, 39]. Increasing evidence suggests that autophagy is activated by various stress, such as ischemia and inflammation and is also closely associated with cardiovascular disease, cancer, and neurodegenerative disorders, especially AD [40–42]. Ohta et al. [43] observed large accumulation of autophagosomes in the dystrophic neuritis both in AD animal models and postmortem brains of AD patients. Furthermore, macroautophagy dysfunction may enhance γ-secretase activity, which in turn increases Aβ by

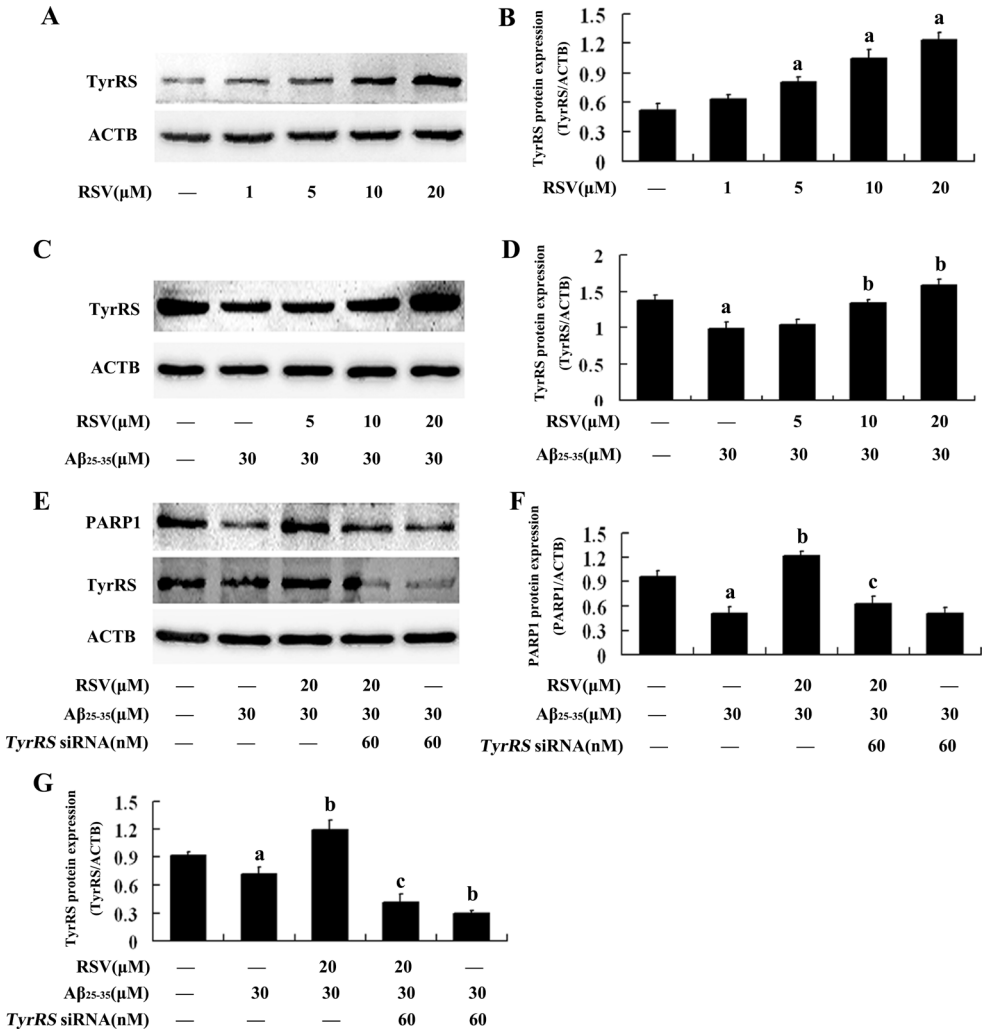

Fig. 5 TyrRS played a key role in RSV-induced PARP1 expression in PC12 cells. **a** PC12 cells were treated with various concentrations (1, 5, 10, and 20 μM) of RSV for 24 h. TyrRS expression was detected by western blot analysis. **b** The *bar graph* shows the quantification of TyrRS. **c** Cells were pretreated with RSV at different concentrations (5, 10, and 20 μM) followed by exposure to $A\beta_{25–35}$ (30 μM) for an additional 24 h. TyrRS expression was detected by western blot analysis. **d** The *bar graph* shows the quantification of TyrRS. **e** Cells were transfected with *TyrRS siRNA* (60 nM) for 5–7 h as described in the "Materials and Methods" section. At 24 h post-transfection, the cells were pretreated with RSV (20 μM) for 2 h and then incubated in the presence or absence of $A\beta_{25–35}$ (30 μM) for an additional 24 h. The expression of TyrRS and PARP1 was determined by western blot analysis. **f**, **g** The *bar graphs* show the quantification of the indicated proteins. Values are presented as mean ± SD (n = 3); $^{a}p < 0.05$; $^{b}p < 0.01$ versus the vehicle-treated control group; $^{c}p < 0.05$; $^{d}p < 0.01$ versus $A\beta_{25–35}$-treated group; $^{*}p < 0.01$ versus RSV and $A\beta_{25–35}$ co-treated group

cleaving the amyloid-β precursor protein. The link between Aβ and autophagy is supported by the direct observation that the autophagosomes contain Aβ and that manipulation of autophagy by genetic or pharmacologic means affects the Aβ pathology of AD model mice [44]. Yuan Tian et al. [45] have shown that the autophagic proteins Atg5, Beclin1, and Ulk1 are involved in the housekeeping clearance of Aβ. Consistent with these results, they observed that in Atg5-knockout MEF cells, as well as in Beclin1 and Ulk1 knocked down cells, Aβ levels were dramatically increased, suggesting that under physiological conditions, Aβ was rapidly cleared by autophagy. Moreover, it has been shown that pharmacological stimulation of autophagy can increase life span in yeast [46, 47], *C. elegans* [48, 49], mice [50] and is beneficial for Aβ induced toxicity in vivo in AD [51, 52]. In addition, our previous studies also demonstrated that RSV improved hepatic steatosis and attenuated endothelial inflammation by inducing autophagy [23, 24]. The current study showed that RSV induced a beneficial autophagic process to prevent $A\beta_{25–35}$-induced neurotoxicity in PC12 cells. Importantly, these findings revealed new insights to elucidate the potential mechanism of the anti-neurotoxicity effect of RSV, in which autophagy may play a critical role.

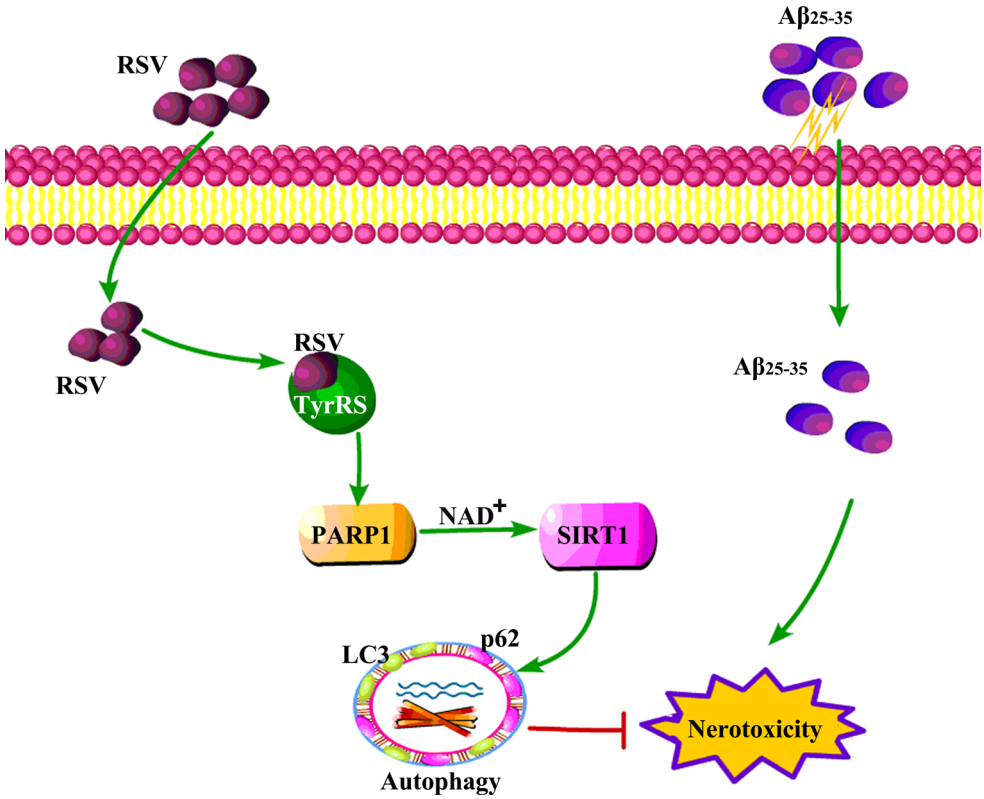

Fig. 6 RSV attenuated $A\beta_{25–35}$-induced neurotoxicity by activating autophagy via the TyrRS-PARP1-SIRT1 signaling pathway

Numerous studies have shown that RSV has obviously beneficial effects on age-related diseases including AD [53–55]. The potential mechanisms underlying the anti-AD activities of RSV have been widely studied and multiple molecular targets of RSV have also been identified, among which SIRT1 was the best-known one [56]. Sirtuins, particularly SIRT1, may play a vital role in protecting neurons from the devastating effects of peroxides, β-amyloid peptides, and nitric oxide [57]. Several studies have indicated that SIRT1 may regulate aging and metabolism in AD. Moreover, SIRT1 down-regulation was found to be associated with Aβ accumulation and disease progression [20, 58, 59]. Recently, Morselli et al. [22] reported that calorie restriction and RSV both promoted extension of lifespan through induction of SIRT1-dependent autophagy. Furthermore, SIRT1 over-expression induces autophagy in both normal growth and starvation conditions, but not in a dominant negative SIRT1 mutant, suggesting that SIRT1 alone is sufficient to induce autophagy even in the presence of nutrients [21]. As demonstrated by our previous studies, RSV induces autophagy in endothelial and liver cells via the activation of SIRT1, thereby attenuating atherosclerosis and nonalcoholic fatty liver disease [23, 24]. Herein, our data revealed that pretreatment with EX527 and *SIRT1* siRNA remarkably inhibited RSV-induced autophagy, suggesting that this process was mainly promoted by triggering endogenous SIRT1 in PC12 cells. In addition, previous studies have shown that SIRT1 acts as a positive regulator of autophagy through modulating the expression of several autophagy-related proteins (Atg5 or Atg7), therefore, RSV might induce autophagy by the regulation of Atg5 or Atg7 expression via SIRT1 activation in $A\beta_{25–35}$-treated PC12 cells. However, the exact underlying mechanisms need to be further elucidated. Moreover, other studies have indicated that RSV is not the direct activator of SIRT1 by showing that RSV indirectly activated SIRT1 through PARP1, a major modulator of NAD^+ metabolism. PARP1 accelerates the biological effects of SIRT1 through increasing the concentration of NAD^+, the rate limiting factor of SIRT1 activity [23]. In the current study, we also found that PARP1 was necessary for SIRT1 activation and autophagy induction stimulated by RSV in PC12 cells. Although, the PARP1-SIRT1 pathway has been tested in some other cell lines treated by RSV, our data, for the first time, confirmed that the PARP1-SIRT1 signaling pathway is crucial for RSV-mediated autophagy in PC12 cells.

In addition to PARP1, our results support an important role for a TyrRS–PARP1-linked pathway in RSV-mediated autophagy in PC12 cells. TyrRS is a homodimer of a 528-amino acid polypeptide and the only higher eukaryotic aminoacyl-tRNA synthetase known to contain an appended eukaryote-specific carboxy (C)-terminal endothelial monocyte–activating polypeptide II–like domain, acting as a general stress transducer [60]. Previous studies have

shown that RSV treatment elicited stress responses and promoted nuclear translocation of endogenous TyrRS in HeLa cells [25, 61]. Furthermore, under stress conditions, nuclear translocation of endogenous TyrRS was concomitant with strong autoPARylation of PARP1 ($PARP1^{PAR}$) [25]. Accordingly, the mechanisms of action of RSV and of the stress response are both linked to the activation of PARP1 through TyrRS. In the present study, we found that RSV protected PC12 cells against $A\beta_{25-35}$-induced toxicity in a TyrRS-dependent manner, which highlights the importance and substantial basis for further studies on phytochemical therapy for AD.

Generally, our findings provided a novel mechanism in which RSV-induced upregulation of autophagy did benefit to $A\beta_{25-35}$ toxicity in neuron cells. Furthermore, the TyrRS-PARP1-SIRT1 signaling pathway was of great importance in regulating RSV-induced autophagy (Fig. 6). Hence, these outcomes open a new avenue of research regarding the potential neurodegenerative protective role of RSV and are significant supplements to the effects of polyphenols on autophagy.

Acknowledgments We are particularly grateful to Dr. Mingliang Chen (Third Military Medical University) for his critical review and valuable suggestions that greatly improved the quality of this manuscript.

Compliance with Ethical Standards

Conflict of interest The authors declare no conflicts of interest.

References

1. Whitehouse PJ, Price DL, Clark AW, Coyle JT, DeLong MR (1981) Alzheimer disease: evidence for selective loss of cholinergic neurons in the nucleus basalis. Ann Neurol 10:122–126
2. Small DH, Cappai R (2006) Alois Alzheimer and Alzheimer's disease: a centennial perspective. J Neurochem 99:708–710
3. Walsh DM, Selkoe DJ (2007) A beta oligomers—a decade of discovery. J Neurochem 101:1172–1184
4. Dong J, Canfield JM, Mehta AK, Shokes JE, Tian B, Childers WS, Simmons JA, Mao Z, Scott RA, Warncke K, Lynn DG (2007) Engineering metal ion coordination to regulate amyloid fibril assembly and toxicity. Proc Natl Acad Sci USA 104:13313–13318
5. Pasinetti GM, Wang J, Ho L, Zhao W, Dubner L (2015) Roles of resveratrol and other grape-derived polyphenols in Alzheimer's disease prevention and treatment. Bba Mol Basis Dis 1852:1202–1208
6. Rege SD, Geetha T, Griffin GD, Broderick TL, Babu JR (2014) Neuroprotective effects of resveratrol in Alzheimer disease pathology. Front Aging Neurosci 6(218):1–12
7. Feng XW, Liang N, Zhu DX, Gao Q, Peng L, Dong HM, Yue QW, Liu HL, Bao LH, Zhang J, Hao J, Gao YM, Yu XJ, Sun JH (2013) Resveratrol inhibits beta-amyloid-induced neuronal apoptosis through regulation of SIRT1-ROCK1 signaling pathway. PloS one 8(3):e59888
8. Baur JA, Sinclair DA (2006) Therapeutic potential of resveratrol: the in vivo evidence. Nat Rev Drug Discov 5:493–506
9. Richard T, Pawlus AD, Iglesias ML, Pedrot E, Waffo-Teguo P, Merillon JM, Monti JP (2011) Neuroprotective properties of resveratrol and derivatives. Ann N Y Acad Sci 1215:103–108
10. Kizilarslanoglu MC, Ulger Z (2015) Role of autophagy in the pathogenesis of Alzheimer disease. Turk J Med Sci 45:998–1003
11. Nixon RA (2007) Autophagy, amyloidogenesis and Alzheimer disease. J Cell Sci 120:4081–4091
12. Zheng L, Marcusson J, Terman A (2006) Oxidative stress and Alzheimer disease: the autophagy connection? Autophagy 2:143–145
13. Pickford F, Masliah E, Britschgi M, Lucin K, Narasimhan R, Jaeger PA, Small S, Spencer B, Rockenstein E, Levine B, Wyss-Coray T (2008) The autophagy-related protein beclin 1 shows reduced expression in early Alzheimer disease and regulates amyloid beta accumulation in mice. J Clin Invest 118:2190–2199
14. Lipinski MM, Zheng B, Lu T, Yan ZY, Py BF, Ng A, Xavier RJ, Li C, Yankner BA, Scherzer CR, Yuan JY (2010) Genome-wide analysis reveals mechanisms modulating autophagy in normal brain aging and in Alzheimer's disease. Proc Natl Acad Sci USA 107:14164–14169
15. Morselli E, Maiuri MC, Markaki M, Megalou E, Pasparaki A, Palikaras K, Criollo A, Galluzzi L, Malik SA, Vitale I, Michaud M, Madeo F, Tavernarakis N, Kroemer G (2010) Caloric restriction and resveratrol promote longevity through the Sirtuin-1-dependent induction of autophagy. Cell Death Dis 1:e10
16. Morselli E, Galluzzi L, Kepp O, Criollo A, Maiuri MC, Tavernarakis N, Madeo F, Kroemer G (2009) Autophagy mediates pharmacological lifespan extension by spermidine and resveratrol. Aging 1:961–970
17. Wang M, Yu T, Zhu C, Sun H, Qiu Y, Zhu X, Li J (2014) Resveratrol triggers protective autophagy through the ceramide/Akt/mTOR pathway in melanoma B16 cells. Nutr Cancer 66:435–440
18. Furuya TK, da Silva PNO, Payao SLM, Rasmussen LT, de Labio RW, Bertolucci PHF, Braga ILS, Chen ES, Turecki G, Mechawar N, Mill J, Smith MDAC (2012) SORL1 and SIRT1 mRNA expression and promoter methylation levels in aging and Alzheimer's Disease. Neurochem Int 61:973–975
19. Sinclair DA (2005) Toward a unified theory of caloric restriction and longevity regulation. Mech Ageing Dev 126:987–1002
20. Julien C, Tremblay C, Emond V, Lebbadi M, Norman S, Bennett DA, Calon F (2009) Sirtuin 1 reduction parallels the accumulation of tau in Alzheimer disease. J Neuropathol Exp Neurol 68:48–58
21. Lee IH, Cao L, Mostoslavsky R, Lombard DB, Liu J, Bruns NE, Tsokos M, Alt FW, Finkel T (2008) A role for the NAD-dependent deacetylase Sirt1 in the regulation of autophagy. Proc Natl Acad Sci USA 105:3374–3379
22. Morselli E, Maiuri MC, Markaki M, Megalou E, Pasparaki A, Palikaras K, Criollo A, Galluzzi L, Malik SA, Vitale I, Michaud M, Madeo F, Tavernarakis N, Kroemer G (2010) Caloric restriction and resveratrol promote longevity through the Sirtuin-1-dependent induction of autophagy. Cell Death Dis 1(1):e10
23. Chen ML, Yi L, Jin X, Liang XY, Zhou Y, Zhang T, Xie Q, Zhou X, Chang H, Fu YJ, Zhu JD, Zhang QY, Mi MT (2013) Resveratrol attenuates vascular endothelial inflammation by inducing autophagy through the cAMP signaling pathway. Autophagy 9:2033–2045
24. Zhang Y, Chen ML, Zhou Y, Yi L, Gao YX, Ran L, Chen SH, Zhang T, Zhou X, Zou D, Wu B, Wu Y, Chang H, Zhu JD, Zhang QY, Mi MT (2015) Resveratrol improves hepatic steatosis by inducing autophagy through the cAMP signaling pathway. Mol Nutr Food Res 59:1443–1457
25. Sajish M, Schimmel P (2015) A human tRNA synthetase is a potent PARP1-activating effector target for resveratrol. Nature 519:370–373

26. Huang TC, Lu KT, Wo YYP, Wu YJ, Yang YL (2011) Resveratrol protects rats from a beta-induced neurotoxicity by the reduction of iNOS expression and lipid peroxidation. PloS one 6(12):e29102
27. Yi L, Jin X, Chen CY, Fu YJ, Zhang T, Chang H, Zhou Y, Zhu JD, Zhang QY, Mi MT (2011) Chemical structures of 4-oxo-flavonoids in relation to inhibition of oxidized low-density lipoprotein (LDL)-induced vascular endothelial dysfunction. Int J Mol Sci 12:5471–5489
28. Chen CY, Yi L, Jin X, Zhang T, Fu YJ, Zhu JD, Mi MT, Zhang QY, Ling WH, Yu B (2011) Inhibitory effect of Delphinidin on monocyte-endothelial cell adhesion induced by oxidized low-density lipoprotein via ROS/p38MAPK/NF-kappa B pathway. Cell Biochem Biophys 61:337–348
29. Pervaiz S, Holme AL (2009) Resveratrol: its biologic targets and functional activity. Antioxid Redox Signal 11:2851–2897
30. Yu JJ, Auwerx J (2009) The role of Sirtuins in the control of metabolic homeostasis. Integr Physiol 1173:E10–E19
31. Wang P, Du H, Zhou CC, Song J, Liu X, Cao X, Mehta JL, Shi Y, Su DF, Miao CY (2014) Intracellular NAMPT-NAD + -SIRT1 cascade improves post-ischaemic vascular repair by modulating Notch signalling in endothelial progenitors. Cardiovasc Res 104:477–488
32. Luo X, Kraus WL (2012) On PAR with PARP: cellular stress signaling through poly(ADP-ribose) and PARP-1. Gene Dev 26:417–432
33. Holtzman DM, Morris JC, Goate AM (2011) Alzheimer's Disease: The Challenge of the Second Century. Sci Transl Med 3(77):77sr1
34. Villaflores OB, Chen YJ, Chen CP, Yeh JM, Wu TY (2012) Curcuminoids and resveratrol as anti-Alzheimer agents. Taiwan J obstet Gynecol 51:515–525
35. Das S, Das DK (2007) Anti-inflammatory responses of resveratrol. Inflammation Allergy Drug Targets 6:168–173
36. Vingtdeux V, Dreses-Werringloer U, Zhao H, Davies P, Marambaud P (2008) Therapeutic potential of resveratrol in Alzheimer's disease. BMC Neurosci 9(Suppl 2):S6
37. Bastianetto S, Menard C, Quirion R (2015) Neuroprotective action of resveratrol. Bba Mol Basis Dis 1852:1195–1201
38. Heeboll S, Thomsen KL, Pedersen SB, Vilstrup H, George J, Gronbaek H (2014) Effects of resveratrol in experimental and clinical non-alcoholic fatty liver disease. World J Hepatol 6:188–198
39. Yu L, Tumati V, Tseng SF, Hsu FM, Kim DN, Hong D, Hsieh JT, Jacobs C, Kapur P, Saha D (2012) DAB2IP regulates autophagy in prostate cancer in response to combined treatment of radiation and a DNA-PKcs inhibitor. Neoplasia 14:1203
40. Ghavami S, Shojaeid S, Yeganeh B, Ande SR, Jangamreddy JR, Mehrpour M, Christoffersson J, Chaabane W, Moghadam AR, Kashani HH, Hashemi M, Owji AA, Los MJ (2014) Autophagy and apoptosis dysfunction in neurodegenerative disorders. Prog Neurobiol 112:24–49
41. Nemchenko A, Chiong M, Turer A, Lavandero S, Hill JA (2011) Autophagy as a therapeutic target in cardiovascular disease. J Mol Cell Cardiol 51:584–593
42. Janku F, McConkey DJ, Hong DS, Kurzrock R (2011) Autophagy as a target for anticancer therapy. Nat Rev Clin Oncol 8:528–539
43. Ohta K, Mizuno A, Ueda M, Li S, Suzuki Y, Hida Y, Hayakawa-Yano Y, Itoh M, Ohta E, Kobori M, Nakagawa T (2010) Autophagy impairment stimulates PS1 expression and gamma-secretase activity. Autophagy 6:345–352
44. Nilsson P, Sekiguchi M, Akagi T, Izumi S, Komor T, Hui K, Sorgjerd K, Tanaka M, Saito T, Iwata N, Saido TC (2015) Autophagy-Related Protein 7 Deficiency in Amyloid beta (A beta) Precursor Protein Transgenic Mice Decreases A beta in the Multivesicular Bodies and Induces A beta Accumulation in the Golgi. Am J Pathol 185:305–313
45. Tian Y, Bustos V, Flajolet M, Greengard P (2011) A small-molecule enhancer of autophagy decreases levels of Abeta and APP-CTF via Atg5-dependent autophagy pathway. Faseb J 25:1934–1942
46. Kaeberlein M, Powers RW 3rd, Steffen KK, Westman EA, Hu D, Dang N, Kerr EO, Kirkland KT, Fields S, Kennedy BK (2005) Regulation of yeast replicative life span by TOR and Sch9 in response to nutrients. Science 310:1193–1196
47. Powers RW 3rd, Kaeberlein M, Caldwell SD, Kennedy BK, Fields S (2006) Extension of chronological life span in yeast by decreased TOR pathway signaling. Genes Dev 20:174–184
48. Jia K, Chen D, Riddle DL (2004) The TOR pathway interacts with the insulin signaling pathway to regulate *C. elegans* larval development, metabolism and life span. Development 131:3897–3906
49. Vellai T, Takacs-Vellai K, Zhang Y, Kovacs AL, Orosz L, Muller F (2003) Genetics: influence of TOR kinase on lifespan in *C. elegans*. Nature 426:620
50. Harrison DE, Strong R, Sharp ZD, Nelson JF, Astle CM, Flurkey K, Nadon NL, Wilkinson JE, Frenkel K, Carter CS, Pahor M, Javors MA, Fernandez E, Miller RA (2009) Rapamycin fed late in life extends lifespan in genetically heterogeneous mice. Nature 460:392–395
51. Spilman P, Podlutskaya N, Hart MJ, Debnath J, Gorostiza O, Bredesen D, Richardson A, Strong R, Galvan V (2010) Inhibition of mTOR by rapamycin abolishes cognitive deficits and reduces amyloid-beta levels in a mouse model of Alzheimer's disease. PLoS ONE 5:e9979
52. Caccamo A, Majumder S, Richardson A, Strong R, Oddo S (2010) Molecular interplay between mammalian target of Rapamycin (mTOR), amyloid-beta, and tau EFFECTS ON COGNITIVE IMPAIRMENTS. J Biol Chem 285:13107–13120
53. Andriambeloson E, Magnier C, Haan-Archipoff G, Lobstein A, Anton R, Beretz A, Stoclet JC, Andriantsitohaina R (1998) Natural dietary polyphenolic compounds cause endothelium-dependent vasorelaxation in rat thoracic aorta. J Nutr 128:2324–2333
54. Lin L, Li J, Lv H, Ma Y, Qian Y (2012) Effect of *Lycium ruthenicum* anthocyanins on atherosclerosis in mice. Zhongguo Zhong Yao Za Zhi 37:1460–1466
55. Wang D, Wei X, Yan X, Jin T, Ling W (2010) Protocatechuic acid, a metabolite of anthocyanins, inhibits monocyte adhesion and reduces atherosclerosis in apolipoprotein E-deficient mice. J Agric Food Chem 58:12722–12728
56. Herskovits AZ, Guarente L (2013) Sirtuin deacetylases in neurodegenerative diseases of aging. Cell Res 23:746–758
57. Kim D, Nguyen MD, Dobbin MM, Fischer A, Sananbenesi F, Rodgers JT, Delalle I, Baur JA, Sui G, Armour SM, Puigserver P, Sinclair DA, Tsai LH (2007) SIRT1 deacetylase protects against neurodegeneration in models for Alzheimer's disease and amyotrophic lateral sclerosis. EMBO J 26:3169–3179
58. Qin WP, Chachich M, Lane M, Roth G, Bryant M, de Cabo R, Ottinger MA, Mattison J, Ingram D, Gandy S, Pasinetti GM (2006) Calorie restriction attenuates Alzheimer's disease type brain amyloidosis in Squirrel monkeys (*Saimiri sciureus*). J Alzheimers Dis 10:417–422
59. Qin WP, Yang TL, Ho L, Zhao Z, Wang J, Chen LH, Zhao W, Thiyagarajan M, MacGrogan D, Rodgers JT, Puigserver P, Sadoshima J, Deng HT, Pedrini S, Gandy S, Sauve AA, Pasinetti GM (2006) Neuronal SIRT1 activation as a novel mechanism

underlying the prevention of Alzheimer disease amyloid neuropathology by calorie restriction. J Biol Chem 281:21745–21754

60. Wakasugi K, Schimmel P (1999) Two distinct cytokines released from a human aminoacyl-tRNA synthetase. Science 284:147–151

61. Viswanathan M, Kim SK, Berdichevsky A, Guarente L (2005) A role for SIR-2.1 regulation of ER stress response genes in determining *C. elegans* life span. Dev Cell 9:605–615